IMA Journal of Applied Mathematics (2001) **66**, 551–566

An illustration of sliding contact at any constant speed on highly elastic half-spaces

L. M. BROCK†
Department of Mechanical Engineering, University of Kentucky, Lexington, Kentucky 40506, USA

AND

H. G. GEORGIADIS
Mechanics Division, National Technical University of Athens, Zographou 15773, Greece

[Received on 15 March 2000; revised on 22 November 2000]

A rigid smooth indentor slides at a constant speed on a compressible isotropic neo-Hookean half-space that is subjected to pre-stress aligned with the surface and sliding direction. A dynamic steady-sliding situation of plane strain is treated as the superposition of contact-triggered infinitesimal deformations superposed upon finite deformations due to pre-stress. The neo-Hookean material behaves for small strains as a linear elastic solid with Poisson's ratio 1 : 4. Exact solutions are presented for both deformations and, for a range of acceptable pre-stress values, the infinitesimal component exhibits the typical non-isotropy induced by pre-stress, and several critical speeds. In view of the unilateral constraints of contact, these speeds serve to define the sliding speed ranges for which physically acceptable solutions arise. A Rayleigh speed is the upper bound for subsonic sliding, and transonic sliding can occur only at a single speed. For the generic parabolic indentor, contact zone traction continuity is lost at the zone leading edge for trans- and supersonic sliding. For pre-stress levels that fall outside the acceptable range, either a negative Poisson effect occurs, or a Rayleigh speed does not exist and the unilateral constraints cannot be satisfied for any subsonic sliding speed.

1. Introduction

Indentation due to rapid sliding contact is an important consideration in mechanism operation, and has been studied (Craggs & Roberts, 1967; Gerstle & Pearsall, 1974; Brock, 1981, 1996) as a dynamic process involving linear elastic solids and rigid indentors. For the case of an arbitrary constant sliding speed it was shown (Brock & Georgiadis, 2000; Georgiadis & Barber, 1993) for sliding, respectively, with and without friction, that solutions may not exist for speeds in various portions of the sub-, trans- and supersonic ranges. A feature of contact in general (Beatty & Usmani, 1975) is that the indented material may be both highly elastic and under pre-stress. This feature was explored for rapid sliding contact (Brock, 1999, 2001). While the sliding speeds were subsonic, the results were consistent with those of Brock & Georgiadis (2000) and Georgiadis & Barber (1993), and did indicate the importance of pre-stress.

†Corresponding author. Email: brock@engr.uky.edu

In this article, the work of Brock (1999, 2001) is extended to include trans- and supersonic sliding speeds. As a specific illustration amenable to tractable solution, a highly elastic half-space is modelled as an isotropic compressible neo-Hookean material subjected to a pre-stress aligned with the surface. A frictionless rigid indentor then translates over the surface at an arbitrary constant speed. Plane-strain steady sliding is assumed, and the process is, after Beatty & Usmani (1975) and Green & Zerna (1968) treated as the superposition of infinitesimal deformations triggered by sliding contact upon the finite deformations due to pre-stress. Some direct notation is used, but Cartesian bases are understood throughout.

2. Basic equations

Consider an elastic body $\Re$ that is homogeneous and isotropic relative to an undisturbed reference configuration κ_0. A smooth motion $\mathbf{x} = \mathbf{x}(\mathbf{X})$ then takes $\Re$ to a deformed equilibrium configuration κ. The Cauchy stress in κ is

$$\mathbf{T} = \alpha_0\mathbf{1} + \alpha_1\mathbf{B} + \alpha_2\mathbf{B}^2, \quad \mathbf{B} = \mathbf{F}\mathbf{F}^T, \quad \mathbf{F} = \frac{\partial \mathbf{x}}{\partial \mathbf{X}}, \tag{1}$$

where $(\alpha_0, \alpha_1, \alpha_2)$ are scalar-valued response functions of the principal invariants (*I,II,III*) of $\mathbf{B}$, and body forces are absent. As noted by Beatty & Usmani (1975), experimentally based inequalities (Truesdell & Noll, 1965) tend to support the restrictions

$$\alpha_0 - II\alpha_2 \leqslant 0, \quad \alpha_1 + I\alpha_2 > 0, \quad \alpha_2 \leqslant 0. \tag{2}$$

An adjacent non-equilibrium configuration κ^* is obtained by superposing an additional, but infinitesimal, displacement $\mathbf{u}$, which depends on $\mathbf{x}$ and time. This requires an additional (incremental) Cauchy stress $\mathbf{T}' = \mathbf{T}^* - \mathbf{T}$, where $\mathbf{T}^*$ is the Cauchy stress in κ^*. To the first order in the displacement gradient $\mathbf{H} = \partial\mathbf{u}/\partial\mathbf{x}$, the components of $\mathbf{T}'$ in the principal reference system, that is, $\mathbf{B} = \mathrm{diag}\{\lambda_1^2, \lambda_2^2, \lambda_3^2\}$, where λ_k are the principal stretches and

$$I = \lambda_1^2 + \lambda_2^2 + \lambda_3^2, \quad II = \lambda_1^2\lambda_2^2 + \lambda_3^2\lambda_1^2 + \lambda_2^2\lambda_3^2, \quad III = \lambda_1^2\lambda_2^2\lambda_3^2 \tag{3}$$

can be written as

$$\begin{bmatrix} T'_{11} \\ T'_{22} \\ T'_{33} \end{bmatrix} = \begin{bmatrix} \lambda'_{11} + 2\mu'_{11} & \lambda'_{12} & \lambda'_{13} \\ \lambda'_{21} & \lambda'_{22} + 2\mu'_{22} & \lambda'_{23} \\ \lambda'_{31} & \lambda'_{32} & \lambda'_{33} + 2\mu'_{33} \end{bmatrix} \begin{bmatrix} H_{11} \\ H_{22} \\ H_{33} \end{bmatrix}, \tag{4a}$$

$$T'_{12} = \mu'_{21}H_{21} + \mu'_{12}H_{12}, \quad T'_{23} = \mu'_{32}H_{32} + \mu'_{23}H_{23}, \quad T'_{31} = \mu'_{13}H_{13} + \mu'_{31}H_{31}. \tag{4b}$$

In (4a, b) the $(\lambda'_{ik}, \mu'_{ik})$ are the generalized Lamé constants defined by

$$\Gamma'_{i1} = \Gamma_{i1}\lambda_1^2, \quad \Gamma'_{i2} = \Gamma_{i2}\lambda_2^2, \quad \Gamma'_{i3} = \Gamma_{i3}\lambda_3^2, \tag{5}$$

where $i = (1, 2, 3)$, the symbol Γ represents either λ or μ, and

$$\tfrac{1}{2}\lambda_{ik} = \frac{\partial\alpha_0}{\partial\lambda_k^2} + \lambda_i^2\frac{\partial\alpha_1}{\partial\lambda_k^2} + \lambda_i^4\frac{\partial\alpha_2}{\partial\lambda_k^2}, \quad \mu_{ik} = \mu_{ki} = \alpha_1 + \alpha_2(\lambda_i^2 + \lambda_k^2). \tag{6}$$

In κ incremental traction boundary conditions on a surface with outwardly-directed normal $\mathbf{n}$ can be written in terms of the traction vector

$$\mathbf{t}^{(n)} = \mathbf{T}'\mathbf{n} + \mathbf{T}\mathbf{n}(\mathbf{n}\cdot\mathbf{H}\mathbf{n}) - \mathbf{T}\mathbf{H}^T\mathbf{n}. \tag{7}$$

Finally, because κ_0 is a homogeneous configuration, the incremental linear momentum balance reduces (Green & Zerna, 1968) to

$$\operatorname{div}\mathbf{T}' = \rho\ddot{\mathbf{u}}, \tag{8}$$

where ρ is the mass density, and $(\cdot)$ denotes the (absolute) time derivative.

3. Compressible neo-Hookean solid

Consider the Hadamard material, which is characterized by the response functions

$$\alpha_0 = 2\sqrt{III}\frac{\mathrm{d}G(III)}{\mathrm{d}III}, \quad \alpha_1 = \frac{1}{\sqrt{III}}(a_0 - Ib_0), \quad \alpha_2 = \frac{b_0}{\sqrt{III}}, \tag{9}$$

where (a_0, b_0) are material constants such that $b_0 = a_0 - \mu$, μ is the shear modulus (Hibbeler, 1997) and $G(1) = 0$. Setting $b_0 = 0$ produces the subclass of isotropic compressible neo-Hookean materials (Beatty & Usmani, 1975), and a simple example of this arises when the form

$$G = \mu\left(\frac{1}{\sqrt{III}} - 1\right) \tag{10}$$

is chosen. This reduces (9) to the one-parameter model

$$\alpha_0 = -\frac{\mu}{III}, \quad \alpha_1 = \frac{\mu}{\sqrt{III}}, \quad \alpha_2 = 0 \tag{11}$$

that satisfies the restrictions (2). For illustration, consider $\Re$ to be a cylindrical bar of circular cross-sectional area A_0 in κ_0 which is placed in a deformed equilibrium state κ under the uniaxial load P. If the bar axis is aligned with the X_1-direction, then the Cauchy stresses in κ are

$$T_{11} = \frac{P}{A}, \quad T_{22} = T_{33} = 0, \quad T_{ik} = 0 \quad (i \neq k), \tag{12}$$

where A is the cross-sectional area in κ, and uniform stress is assumed. Because $\mathbf{X}$ gives the principal directions with stretches λ_1 and $\lambda_2 = \lambda_3 = \lambda_T$, equations (1), (3) and (11) combine to give

$$\frac{P}{A} = \mu\left(\lambda_1^{3/2} - \frac{1}{\lambda_1}\right), \quad \lambda_T = \frac{1}{\lambda_1^{1/4}}. \tag{13}$$

Because $A = \lambda_T^2 A_0$ for homogeneous deformation and $\lambda_1 = 1 + e_1$, where e_1 is the axial unit extension of the bar, $(13)_1$ can be rewritten as

$$\frac{P}{A_0} = \mu\left[1 + e_1 - \frac{1}{(1+e_1)^{3/2}}\right]. \tag{14}$$

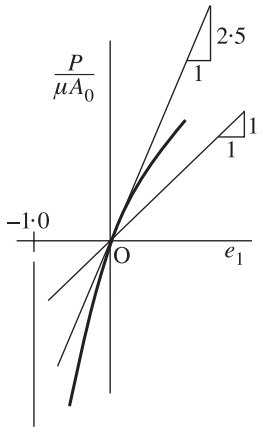

FIG. 1. Compressible neo-Hookean material response in axial loading.

Equation (14) relates a first Piola–Kirchoff stress to unit extension, which is a standard objective of the simple tension test (Hibbeler, 1997). A schematic of (14) is given in Fig. 1, and the effective Young's modulus and Poisson's ratio (E_e, ν_e) follow from $(13)_2$ and the slope of (14) as

$$E_e = \mu\left[1 + \frac{3}{2(1+e_1)^{5/2}}\right], \quad \nu_e = -\frac{\lambda_T - 1}{\lambda_1 - 1} = \frac{(1+e_1)^{1/4} - 1}{e_1(1+e_1)^{1/4}}. \tag{15}$$

Clearly $E_e \to \mu$ for large extensions, but $E_e \to 2{\cdot}5\mu$ when they are small. This small-extension behaviour corresponds to a Young's modulus in an isotropic linear elastic solid with Poisson's ratio 1 : 4 (Hibbeler, 1997) and indeed, $(15)_2$ gives this value when $e_1 \to 0$.

4. Sliding contact problem

Consider that $\Re$ in κ_0 occupies a half-space defined in terms of a fixed Cartesian basis as the region $X_2 > 0$. The smooth motion

$$x_1 = \lambda_1 X_1, \quad x_2 = \lambda_2 X_2, \quad x_3 = X_3 \tag{16}$$

takes $\Re$ into the plane-strain equilibrium state κ defined by

$$T_{11} = \sigma_1, \quad T_{22} = 0, \quad \lambda_3 = 1, \tag{17}$$

where σ_1 is a known constant (pre)-stress. Now $\Re$ occupies the half-space $x_2 > 0$, and (x_k, λ_k) are the principal coordinates and stretches. For the compressible neo-Hookean model (11), equations (1), (3), (16) and (17) combine to give

$$\begin{aligned} &\lambda_2 = \frac{1}{\omega^{1/4}}, \quad \lambda_1 = \omega\lambda_2, \quad \omega = \frac{\sigma_1}{2\mu} + \sqrt{1 + \left(\frac{\sigma_1}{2\mu}\right)^2}, \\ &T_{33} = \mu\left(\frac{1}{\sqrt{\omega}} - \frac{1}{\omega}\right), \quad T_{ik} = 0 \quad (i \neq k), \end{aligned} \tag{18}$$

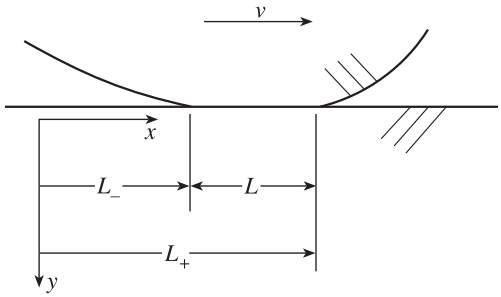

FIG. 2. Schematic of sliding contact process.

where $0 < \omega \leqslant 1 (\sigma_1 \leqslant 0)$ and $\omega \geqslant 1 (\sigma_1 \geqslant 0)$. Equations (16)–(18) describe $\Re$ in κ.

For any superposed infinitesimal deformation $\kappa \to \kappa^*$ of $\Re$, the incremental stresses are given by (4a, b) where, in view of (5), (6), (17) and (18),

$$\begin{aligned} &\lambda'_{1k} = \mu\left(\frac{2}{\omega} - \omega\right), \quad \lambda'_{2k} = \mu'_{k2} = \frac{\mu}{\omega}, \\ &\lambda'_{3k} = \mu\left(\frac{2}{\omega} - \frac{1}{\sqrt{\omega}}\right), \quad \mu'_{k1} = \mu\omega, \quad \mu'_{k3} = \frac{\mu}{\sqrt{\omega}}. \end{aligned} \tag{19}$$

Here $k = 1, 2, 3$ and it is noted that all the constants are positive so long as

$$0 < \omega < \sqrt{2} \quad \left(\sigma_1 < \frac{\mu}{\sqrt{2}}\right). \tag{20}$$

In this article, the infinitesimal deformation occurs when a frictionless rigid indentor of infinite length and invariant profile in the x_3-direction is simultaneously pressed into the half-space surface $x_2 = 0$ with compressive force (per unit of length) N, and translated parallel to that surface in the positive x_1-direction with a constant speed v. Eventually a dynamic plane-strain situation of steady sliding is reached, as shown by the schematic of Fig. 2. As indicated there, it is convenient to introduce the coordinates (x, y, z) that correspond to (x_1, x_2, x_3), but which translate parallel to the surface with the indentor. Then, the boundary conditions for $\Re$ along $y = 0$ are

$$\mathbf{t}^{(-2)} = 0 \quad (x \notin L); \quad t_1^{(-2)} = t_3^{(-2)} = 0, \quad u_2 = U(x) \quad (x \in L) \tag{21}$$

where, as depicted in Fig. 2, $x = L_\pm$ locate the leading and trailing edges of the indentor contact zone. The symbol L is used to represent both the contact zone itself and its length $L = L_+ - L_-$. The function $U(x)$ is the normal motion imposed by the indentor profile in the contact zone. In view of (16), the total and superposed normal displacements along $y = 0$ are the same. The constants $L_\pm$ are *a priori* unknown.

Because the process is one of steady sliding in plane-strain, only the components (u_1, u_2) of the superposed displacements arise, and these depend only on (x, y). Moreover, time derivatives in the absolute (inertial) frame reduce to the form $-v\partial()/\partial x$. Thus, in light of (4a, b), (8) and (19), the relevant governing field equations for $y > 0$ for the superposed

deformation are

$$\begin{aligned} &\frac{1}{\omega}\frac{\partial^2 u_1}{\partial y^2} + \left(\frac{2}{\omega} + \omega - c^2\right)\frac{\partial^2 u_1}{\partial x^2} + \frac{2}{\omega}\frac{\partial^2 u_2}{\partial x \partial y} = 0, \\ &\frac{2}{\omega}\frac{\partial^2 u_1}{\partial x \partial y} + \frac{3}{\omega}\frac{\partial^2 u_2}{\partial y^2} + (\omega - c^2)\frac{\partial^2 u_2}{\partial x^2} = 0, \end{aligned} \tag{22}$$

where the non-zero elements of $\mathbf{T}'$ are defined by the constitutive formulae

$$\begin{aligned} &\frac{1}{\mu}T'_{11} = \left(\frac{2}{\omega} + \omega\right)\frac{\partial u_1}{\partial x} + \left(\frac{2}{\omega} - \omega\right)\frac{\partial u_2}{\partial y}, \quad \frac{1}{\mu}T'_{22} = \frac{1}{\omega}\frac{\partial u_1}{\partial x} + \frac{3}{\omega}\frac{\partial u_2}{\partial y}, \\ &\frac{1}{\mu}T'_{12} = \omega\frac{\partial u_2}{\partial x} + \frac{1}{\omega}\frac{\partial u_1}{\partial y}, \quad \frac{1}{\mu}T'_{33} = \left(\frac{2}{\omega} - \frac{1}{\sqrt{\omega}}\right)\left(\frac{\partial u_1}{\partial x} + \frac{\partial u_2}{\partial y}\right). \end{aligned} \tag{23}$$

Here c is the sliding speed non-dimensionalized with respect to the classical (rest) value (Achenbach, 1973) of the rotational wave speed, that is,

$$c = \frac{v}{v_r}, \quad v_r = \sqrt{\frac{\mu}{\rho}}. \tag{24}$$

Equation $(23)_1$ indicates that extensional strain associated with the x-direction is independent of transverse loading when ω achieves a critical value $\omega = \sqrt{2}$, cf. (20). Indeed, for ω exceeding that value, $(23)_1$ implies a negative Poisson effect. Moreover, (23) shows that $\operatorname{tr}\mathbf{T}'$ and $\operatorname{tr}\mathbf{H}$ are not directly proportional. This indicates the typical (Green & Zerna, 1968) result that the superposed deformations are governed by equations analogous to those for a non-isotropic body, although $\Re$ in κ_0 is isotropic.

The mixed boundary conditions along $y = 0$ for this deformation can in view of (5), (17) and (18) be extracted from (21) as

$$T'_{12} - \sigma_1\frac{\partial u_2}{\partial x} = 0; \quad T'_{22} = 0 \quad (x \notin L), \quad \frac{\partial u_2}{\partial x} = \frac{\mathrm{d}U(x)}{\mathrm{d}x} \quad (x \in L). \tag{25}$$

Equations (25) reflect the fact that $t_3^{(-2)}$ vanishes identically and that the steady-state nature of the superposed deformation allows a solution only to within an arbitrary rigid-body motion. In addition, we expect the T'_{ik} in (23) to vanish when $\sqrt{x^2 + y^2} \to \infty$, $y > 0$ and to be non-singular and continuous almost everywhere. This latter requirement, as well as the assumption implicit in Fig. 2 and (25), that multiple contact zones (Brock, 1996) do not in fact arise, can be justified in part by requiring that $(U, \mathrm{d}U/\mathrm{d}x, \mathrm{d}^2U/\mathrm{d}x^2)$ be finite and continuous for $x \in L$. Then, the resultant of T'_{22} on the contact zone should be the specified compressive force $-N$, and the contact zone parameters $L_\pm$ must be determined as part of the solution. Finally, two unilateral constraints (Georgiadis & Barber, 1993) must hold: (a) contact zone normal stress is non-tensile, and (b) indentor and half-space surfaces do not interpenetrate.

5. Candidates for superposed solutions

Following the standard (Erdogan, 1976) practice for two-dimensional mixed boundary-value problems in classical elasticity, the solution for the superposed deformation is

obtained by first considering the same equations (22)–(24) and boundedness/continuity conditions, but with (25) replaced by the unmixed conditions

$$T'_{12} - \sigma_1 \frac{\partial u_2}{\partial x} = 0, \quad T'_{22} = \sigma(x) \tag{26}$$

along $y = 0$, where $\sigma(x)$ represents the contact zone traction; it must vanish identically for $x \notin L$, and should be continuous at $x = L_\pm$. The solution to this simpler problem will be the superposed solution if a $\sigma(x)$ can be found such that $(25)_3$ is also satisfied.

In the Appendix, solutions to (22)–(24) and (26) are obtained by use of integral transform techniques (van der Pol & Bremmer, 1950). In light of the results $(A.8)_2$ there, the condition $(25)_3$ is reduced in the case of subsonic $(0 < c < c_b)$ sliding to the equation

$$-\frac{\sqrt{\omega} K_0 a}{\mu \pi R}(P)\int_L \frac{\sigma(t)\,\mathrm{d}t}{t - x} = \frac{\mathrm{d}U(x)}{\mathrm{d}x} \quad (x \in L), \tag{27}$$

where, as noted in the Appendix, $(v_r c_a, v_r c_b)$ are dilatational and rotational wave speeds in κ^*, and

$$c_b = \sqrt{\omega}, \quad c_a = \sqrt{\omega + \frac{2}{\omega}} > c_b. \tag{28}$$

To obtain (27) from $(A.8)_2$, use has been made of the result (Carrier & Pearson, 1988)

$$\frac{k}{(t - x)^2 + k^2} \to \pi \delta(t - x) \quad (k \to 0+), \tag{29}$$

where $\delta(\,)$ is the Dirac function, the definition (A.3a) for (a, R), and the definition

$$K_0 = c^2 - \omega + \frac{1}{\omega}. \tag{30}$$

As in the Appendix, L in the integral symbol indicates integration over the real interval (L_-, L_+), while (P) signifies that integration is in the Cauchy principal value sense. Equation (27) is a standard Cauchy integral equation (Erdogan, 1976) whose solution is

$$\sigma(x) = \frac{\mu R}{\sqrt{\omega} K_0 a}\sqrt{\frac{x - L_-}{L_+ - x}}\frac{1}{\pi}(P)\int_L \frac{\mathrm{d}U(t)}{\mathrm{d}t}\sqrt{\frac{L_+ - t}{t - L_-}}\frac{\mathrm{d}t}{t - x} \quad (x \in L). \tag{31}$$

Equation (31) is appropriately bounded as $x \to L_-$, but boundedness as $x \to L_+$ occurs only when

$$\int_L \frac{\mathrm{d}U(t)}{\mathrm{d}t}\frac{\mathrm{d}t}{\sqrt{t - L_-}\sqrt{L_+ - t}} = 0. \tag{32}$$

This requirement serves as one equation for determining the contact zone parameters $L_\pm$. The other equation arises from the requirement that $-N$ be the resultant of T'_{22} on the contact zone. That is,

$$\int_L \sigma(x)\,\mathrm{d}x = -N. \tag{33}$$

Substitution of (31) into (33) and performing the x-integration with standard (Gradshteyn & Ryzhik, 1980) tables gives the more explicit condition

$$\frac{\mu R}{\sqrt{\omega}K_0 a}\int_L \frac{\mathrm{d}U(t)}{\mathrm{d}t}\sqrt{\frac{L_+ - t}{t - L_-}}\,\mathrm{d}t = N. \tag{34}$$

For sliding in the transonic ($c_b < c < c_a$) speed range, the result $(A.9)_2$ reduces $(25)_3$ to the Cauchy integral equation

$$-\frac{\sqrt{\omega}a}{\mu D}\left[\frac{4a\beta}{\omega}\sigma(x) + \frac{K^2}{\pi}(P)\int_L \frac{\sigma(t)\,\mathrm{d}t}{t - x}\right] = \frac{\mathrm{d}U(x)}{\mathrm{d}x} \quad (x \in L), \tag{35}$$

where β is defined by (A.10) and

$$D = \left(\frac{2}{\omega} - K\right)\left(K^2 - \frac{4}{3\omega^2}\right). \tag{36}$$

Following Erdogan (1976), the solution to (35) is

$$\sigma(x) = -\frac{\mu D}{\sqrt{\omega}a} I\left(\frac{\mathrm{d}U}{\mathrm{d}x}; x\right) \quad (x \in L), \tag{37}$$

where the operator I and eigenvalue υ are defined by

$$I(g; x) = g(x)\cos\pi\upsilon + \frac{1}{\pi}\left(\frac{L_+ - x}{x - L_-}\right)^{\upsilon}\sin\pi\upsilon(P)\int_L g(t)\left(\frac{t - L_-}{L_+ - t}\right)^{\upsilon}\frac{\mathrm{d}t}{t - x} \quad (x \in L),$$
$$\upsilon = \frac{1}{\pi}\tan^{-1}\frac{4a\beta}{\omega K^2} - \frac{1}{2} \quad (-\tfrac{1}{2} < \upsilon < 0). \tag{38}$$

The counterparts to the auxiliary conditions (32) and (34) are

$$\int_L \frac{\mathrm{d}U(t)}{\mathrm{d}t}\left(\frac{t - L_-}{L_+ - t}\right)^{\upsilon}\frac{\mathrm{d}t}{t - L_+} = 0, \quad -\frac{\mu D}{\sqrt{\omega}a}\int_L \frac{\mathrm{d}U(t)}{\mathrm{d}t}\left(\frac{t - L_-}{L_+ - t}\right)^{\upsilon}\mathrm{d}t = N. \tag{39}$$

Finally, for sliding speeds in the supersonic ($c > c_a$) range, $(A.11)_2$ and $(25)_3$ lead immediately to the results

$$\sigma(x) = \frac{\mu R_+}{\sqrt{\omega}K_0\alpha}\frac{\mathrm{d}U(x)}{\mathrm{d}x} \quad (x \in L),$$
$$\frac{\mu R_+}{\sqrt{\omega}K_0\alpha}[U(L_-) - U(L_+)] = N, \tag{40}$$

where (α, R_+) are defined by (A.12) and, in this case, boundedness at $x = L_\pm$ is controlled more directly by the form of $U(x)$. The translational part of any rigid body motion cancels out in $(40)_2$.

Equations (31), (37) and $(40)_1$, together with their auxiliary conditions, constitute in light of, respectively, (A.8), (A.9) and (A.11), the solution candidates for the superposed infinitesimal deformations. The actual solutions are those that satisfy in addition the unilateral constraints (a) and (b).

6. Superposed solution: subsonic case

To illustrate the solution identification process for subsonic ($0 < c < c_b$)sliding speeds, the generic parabolic indentor is treated. That is,

$$U(x) = U_0 + U_1 x + \tfrac{1}{2} U_2 x^2, \tag{41}$$

where the U_k are real constants. Substitution of (41) into (31), (32) and (34) gives, upon integration by means of standard tables (Gradshteyn & Ryzhik, 1980),

$$\sigma(x) = \frac{\mu R U_2}{\sqrt{\omega} K_0 a} \sqrt{L_+ - x} \sqrt{x - L_-} \quad (x \in L), \tag{42}$$

where $L_\pm$ can be obtained from the formulae

$$2U_1 + (L_+ + L_-)U_2 = 0, \quad -\frac{\pi \mu R U_2 L^2}{8\sqrt{\omega} K_0 a} = N. \tag{43}$$

In view of $(26)_2$, the unilateral constraint (a) requires that $\sigma(x) \leqslant 0$, which, as indicated by (42), implies the condition $U_2 R / K_0 \leqslant 0$.

Study of (A.3a, b) shows that the dimensionless quantity R has roots $c = \pm(c_0, c_R)$, where

$$c_0 = \sqrt{\omega - \frac{1}{\omega}}, \quad c_R = \sqrt{\omega + \frac{1}{\omega}\left(1 - \frac{2}{\sqrt{3}}\right)}. \tag{44}$$

For $\sqrt{2/\sqrt{3} - 1} < \omega < \sqrt{2}$, the second root is real and $0 < c_R < c_b$. Therefore, $v = v_r c_R$ is a critical sliding speed, at which the solution to (27) is undefined; it plays the role of the Rayleigh speed (Achenbach, 1973). Indeed, R as defined by (A.3a) has a form similar to that of the classical Rayleigh function. For $0 < \omega < \sqrt{2/\sqrt{3} - 1}$, however, the second root is imaginary, and so has no meaning as a wave speed. In light of $(18)_1$, these observations imply that a Rayleigh wave does not exist when

$$\sigma_1 < \sigma_c, \quad \sigma_c = -2\mu(\sqrt{3} - 1)\sqrt{\frac{2}{\sqrt{3}} + 1}. \tag{45}$$

In view of (44), the first root is imaginary for all $0 < \omega < 1$ ($\sigma_1 < 0$), and so does not correspond to a wave speed. For $1 < \omega < \sqrt{2}$ ($0 < \sigma_1 < \mu/\sqrt{2}$), however, it is real and $0 < c_0 < c_R$. Nevertheless, no critical sliding speed seems to arise in this case, because (30) shows that $c = \pm c_0$ are also roots of the dimensionless quantity K_0. Indeed, in the light of (A.3a, b) and (30), it can be shown that, for $\sigma_1 > \sigma_c$,

$$\frac{R}{K_0} \begin{cases} > 0 & (0 < c < c_R), \\ < 0 & (c_R < c < c_b), \end{cases} \tag{46a}$$

and for $\sigma_1 < \sigma_c$,

$$\frac{R}{K_0} < 0 \quad (0 < c < c_b). \tag{46b}$$

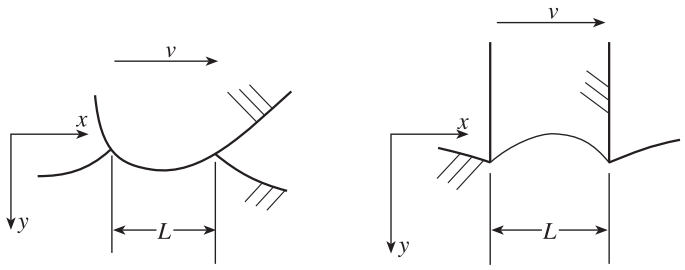

FIG. 3. (a) Surface deformation schematic for acceptable solution. (b) Surface deformation schematic for artificial solution.

If $(46a)_1$ governs, one must have $U_2 < 0$. In view of Fig. 2, this means that the sliding indentor is concave upwards. The cases $(46a)_2$ and (46b) require, however, that $U_2 > 0$, that is, the indentor is concave downward. Although the former situation seems more physically acceptable, imposition of unilateral constraint (b) provides closure.

It is noted that (42) is both bounded and continuous (vanishes) at the contact zone edges $x = L_{\pm}$. Study of (A.8) shows that this, in turn, guarantees continuity of $(\partial u_1/\partial x, \partial u_2/\partial x)$ at the edges. However, taking the derivative of $(A.8)_2$ and then letting $y = 0$ gives in light of $(43)_2$ an integral that can be performed with standard tables (Gradshteyn & Ryzhik, 1980):

$$\frac{\partial^2 u_2}{\partial x^2} = U_2 \left[1 - \frac{1}{2} \left(\sqrt{\frac{x - L_-}{x - L_+}} + \sqrt{\frac{x - L_+}{x - L_-}} \right) \right] \quad (x \notin L). \tag{47}$$

This is approximately the curvature of the half-space surface outside the contact zone. For $U_2 < 0$, (47) behaves as $(+\infty, x \to L_{\pm})$, which implies the schematic in Fig. 3a for the deformed surface. For $U_2 > 0$, however, (47) behaves as $(-\infty, x \to L_{\pm})$, which suggests interpenetration—thereby violating unilateral constraint (b)—unless the artifice depicted in Fig. 3b is adopted, which treats the indentor dimensions as *a priori* defined by the parameters $L_{\pm}$.

In summary, then, for pre-stress below a critical compressive value, the deformed configuration exhibits a critical speed of the Rayleigh type that serves as an upper bound for sliding contact in the subsonic case, that is, $0 < v < v_r c_R$. This behaviour is analogous to that for a linear elastic solid (Georgiadis & Barber, 1993). For pre-stress that exceeds the critical value in compression, subsonic steady sliding cannot occur.

7. Superposed solution: transonic case

For transonic $(c_b < c < c_a)$ sliding speeds, the form (41) is again used to illustrate the solution specification process. In this instance, (37), (39) and the use of standard tables (Gradshteyn & Ryzhik, 1980) give the bounded and continuous formula

$$\sigma(x) = \frac{\mu D U_2}{\sqrt{\omega a}} (L_+ - x)^{1+\upsilon} (x - L_-)^{-\upsilon} \quad (x \in L). \tag{48}$$

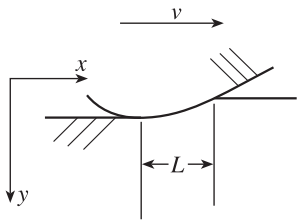

FIG. 4. Surface deformation schematic for trans- and supersonic sliding speeds.

Equations (30) and (36) show that $D < 0$ for all $c_b < c < c_a$. This implies in light of the subsonic sliding analysis that unilateral constraint (a) can only be satisfied if $U_2 > 0$. Consequently, it would appear that constraint (b) cannot be satisfied for any transonic sliding speed unless the situation depicted in Fig. 3b is adopted.

However, (A.3a) shows that $K(\pm c_K) = 0$, where

$$c_K = \sqrt{\omega + \frac{1}{\omega}} \quad (c_b < c_K < c_a) \tag{49}$$

and when $c = c_K$, (38) gives $\upsilon = 0$ and (37) reduces to the degenerate case

$$\sigma(x) = \frac{2\mu}{\omega}\frac{\mathrm{d}U(x)}{\mathrm{d}x} \quad (x \in L). \tag{50}$$

For the case (41), it can be shown that (50) gives the form

$$\sigma(x) = \frac{2\mu U_2}{\omega}(x - L_-) \quad (x \in L) \tag{51}$$

which satisfies both unilateral constraints when $U_2 < 0$ and the conditions

$$U_1 + U_2 L_- = 0, \quad -\frac{\mu U_2 L^2}{\omega} = N. \tag{52}$$

Equation (52) can be used to obtain the contact zone parameters $L_\pm$ but, unlike its subsonic counterpart (43), does not guarantee continuity of $\sigma(x)$ at $x = L_+$, that is, (50) gives a finite discontinuity at the contact zone leading edge. A schematic of the surface deformation in Fig. 4 shows that (51) locates the contact zone trailing edge $x = L_-$ at the point of zero indentor slope, that is, the point of maximum normal surface displacement under the indentor.

8. Superposed solutions: supersonic case

For supersonic ($c > c_a$) sliding speeds, combining (41) with (40) and then imposing both unilateral constraints gives

$$\sigma(x) = \frac{\mu R_+ U_2}{\sqrt{\omega} K_0 \alpha}(x - L_-) \quad (x \in L), \tag{53}$$

where $U_2 < 0$ and $L_\pm$ are determined from the formulae

$$U_1 + U_2 L_- = 0, \quad -\frac{\mu R_+ U_2 L^2}{2\sqrt{\omega} K_0 \alpha} = N. \tag{54}$$

Equation (53) shows that, as in the transonic case ($c = c_K, c_b < c_K < c_a$), the contact zone traction becomes discontinuous at the leading ($x = L_+$) edge. Again, Fig. 4 depicts the surface deformation, and (54) locates the contact zone trailing edge $x = L_-$ at the point of maximum normal surface displacement under the indentor.

9. Comments

This article reported on rapid sliding contact on a pre-stressed highly elastic half-space. The sliding indentor was frictionless, could in principle slide at any constant speed, and the pre-stress was aligned with the half-space surface and sliding direction. The half-space was modelled as an isotropic compressible neo-Hookean material that, for small stresses, behaved as a linear elastic solid with Poisson's ratio 1 : 4.

The dynamic analysis treated the process as a plane-strain problem of steady sliding, and the problem solutions as the superposition of infinitesimal deformations triggered by the sliding contact upon the finite deformations due to pre-stress. Exact solutions were obtained for both deformations; in particular, the mixed boundary-value problem for the infinitesimal deformation was solved by combining integral transform and Cauchy integral equation solution techniques. Boundedness requirements on the contact zone traction gave rise to auxiliary conditions that allowed the contact edge locations to be determined as well.

As is typical (Green & Zerna, 1968), the pre-stress induced a *de facto* non-isotropy in the infinitesimal solution response, and equations (28) and (44) showed that the associated wave speeds (rotational, dilatational, Rayleigh) are sensitive to pre-stress. In particular, (44) showed that the Rayleigh wave disappears for pre-stresses that exceed the critical value $2\mu(\sqrt{3}-1)\sqrt{2/\sqrt{3}+1}$ in compression, where μ is the shear modulus. A plot of the speeds (c_b: rotational, c_a: dilatational, c_R: Rayleigh), non-dimensionalized with respect to the rest value of the rotational wave speed, versus pre-stress is given in Fig. 5. It is seen that increasing a compressive pre-stress lowers the rotational and Rayleigh wave speeds, but increases the dilatational wave speed. A critical tensile pre-stress also exists; for values greater than $\mu/\sqrt{2}$, the infinitesimal deformation exhibits a negative Poisson effect. Both critical stresses are of $O(\mu)$, but may be relevant within the context of highly elastic response.

The aforementioned mixed boundary-value problems actually produced only candidate solutions. The actual solutions need in addition to satisfy the standard unilateral constraints of contact, which preclude tensile contact zone traction and indentor/half-space interpenetration. Imposition of these conditions for the case of the generic parabolic indentor showed that physically acceptable steady sliding contact can occur only at (1) sliding speeds below the Rayleigh wave speed, (2) a particular speed in the transonic range and (3) all supersonic sliding speeds. Figure 5 also exhibits the variation with pre-stress of the non-dimensionalization c_K of the single allowable transonic speed. While the contact zone traction was finite in all three cases, continuity at the contact zone leading

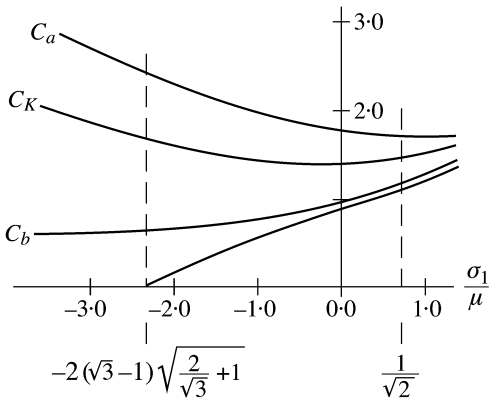

FIG. 5. Non-dimensionalized speeds versus pre-stress.

edge was maintained only for case (1). Moreover, the trailing edge of the contact zone in cases (2) and (3) corresponded to the point of maximum normal surface displacement under the indentor.

Because the Rayleigh wave disappears at a critical compressive pre-stress, case (1) indicates that subsonic sliding contact cannot occur for compressive pre-stresses above that level. While, as noted above, both critical pre-stresses are high, the present result does indicate, in view of Fig. 5, that a compressive pre-stress inhibits steady sliding contact at subsonic speeds.

The results obtained here are consistent with those of Georgiadis & Barber (1993), which dealt with frictionless sliding contact in a linear elastic solid with no pre-stress, and focused in part on the moving point force problem. The study by Brock & Georgiadis (2000) considered the effects of friction at all possible constant sliding speeds, but pre-stress was not involved, and the solid was a linear thermoelastic material. Thermoelastic coupling required, moreover, the use of robust asymptotic solutions. The results from the present analysis are, therefore, being extended to include friction and coupled thermoelasticity.

Acknowledgement

The support of NATO grant CRG 972116 facilitated preliminary discussions of this work, through a visit by the first author to the National Technical University of Athens.

REFERENCES

ACHENBACH, J. D. 1973 *Wave Propagation in Elastic Solids*. Amsterdam: North–Holland.

BEATTY, M. F. & USMANI, S. A. 1975 On the indentation of a highly elastic half-space. *Q. Jl Mech. Appl. Math.*, **28**, 47–62.

BROCK, L. M. 1981 Sliding and indentation by a rigid half-wedge with friction and displacement coupling. *Int. J. Eng. Sci.*, **19**, 33–40.

BROCK, L. M. 1996 Some analytical results for heating due to irregular sliding contact. *Indian J. Pure Appl. Math.*, **27**, 1257–1278.

BROCK, L. M. 1999 Rapid sliding indentation with friction of a pre-stressed thermoelastic material. *J. Elast.*, **53**, 161–188.

BROCK, L. M. 2001 Rapid sliding contact on a highly elastic pre-stressed material. *Int. J. Non-Linear Mech.*, **36**, 433–442.

BROCK, L. M. & GEORGIADIS, H. G. 2000 Sliding contact with friction of a thermoelastic solid at subsonic, transonic and supersonic speeds. *J. Therma. Stresses*, **23**, 629–656.

CARRIER, G. F. & PEARSON, C. E. 1988 *Partial Differential Equations*. New York: Academic Press.

CRAGGS, J. W. & ROBERTS, A. M. 1967 On the motion of a heavy cylinder over the surface of an elastic half-space. *ASME. J. Appl. Mech.*, **24**, 207–209.

ERDOGAN, F. 1976 Mixed boundary-value problems in mechanics. *Mechanics Today*, Vol. 4. (S. Nemat-Nasser, ed.), New York: Pergamon Press.

GEORGIADIS, H. G. & BARBER, J. R. 1993 On the super-Rayleigh/subseismic elastodynamic indentation problem. *J. Elast.*, **31**, 141–161.

GERSTLE, F. P. & PEARSALL, G. W. 1974 The stress response of an elastic surface to a high-velocity, unlubricated punch. *ASME. J. Appl. Mech.*, **41**, 1036–1040.

GRADSHTEYN, I. S. & RYZHIK, I. M. 1980 *Table of Integrals, Series and Products*. New York: Academic Press.

GREEN, A. W. & ZERNA, W. 1968 *Theoretical Elasticity*, 2nd edn. London: Oxford University Press.

HIBBELER, R. C. 1997 *Mechanics of Materials*, 3rd edn. Saddle River, NJ: Prentice-Hall.

TRUESDELL, C. T. & NOLL, W. 1965 The non-linear field theories of mechanics. *Handbuch der Physik* Vol. III/3. Berlin: Springer.

VAN DER POL, B. & BREMMER, H. 1950 *Operations Based on the Two-sided Laplace Integral*. Cambridge: Cambridge University Press.

Appendix

Consider the bilateral Laplace transform (van der Pol & Bremmer, 1950) and inverse

$$\hat{F} = \int_{-\infty}^{\infty} F(x)\mathrm{e}^{-px}\mathrm{d}x, \quad F(x) = \frac{1}{2\pi \mathrm{i}} \int \hat{F}\mathrm{e}^{px}\,\mathrm{d}p, \tag{A.1}$$

where p is imaginary and integration in $(A.1)_2$ is along a Bromwich contour in the p-plane. Application of $(A.1)_1$ to (22) and (26) in view of (23) and the boundedness requirements gives a coupled set of linear ordinary differential equations that can be solved in terms of the transform of the contact zone normal traction $\sigma(x)$. The results are

$$\begin{bmatrix} \hat{u}_1 \\ \sqrt{p}\hat{u}_2 \end{bmatrix} = \frac{\hat{\sigma}}{\mu p R} \begin{bmatrix} -K & -2ab \\ a\sqrt{\omega}K\sqrt{-p} & \dfrac{2a}{\omega}\sqrt{-p} \end{bmatrix} \begin{bmatrix} \mathrm{e}^{-\sqrt{\omega}ay\sqrt{p}\sqrt{-p}} \\ \mathrm{e}^{-\sqrt{\omega}by\sqrt{p}\sqrt{-p}} \end{bmatrix} \tag{A.2}$$

for $y > 0$, where

$$\sqrt{3}a = \sqrt{c^2 - c_a^2}, \quad b = \sqrt{c^2 - c_b^2}, \quad K = c^2 - \omega - \frac{1}{\omega}, \quad R = \frac{4}{\omega}ab - K^2, \tag{A.3a}$$

$$c_b = \sqrt{\omega}, \quad c_a = \sqrt{\omega + \frac{2}{\omega}} > c_b, \tag{A.3b}$$

the dimensionless sliding speed c is defined in (24), and

$$\hat{\sigma} = \int_L \sigma(t)\mathrm{e}^{-pt}\,\mathrm{d}t. \tag{A.4}$$

The dimensionless constants in (A.3b) define rotational ($v_r c_b$) and dilatational ($v_r c_a$) wave speeds in the deformed configuration. In (A.4) the symbol L affixed to the integral operator signifies that integration is over the real interval (L_-, L_+). Integration by parts indicates that the terms $p\hat{u}_k$ in (A.2) are the transforms of $\partial u_k/\partial x$. In light of the fact that non-transient displacements can be found only to within an arbitrary rigid-body motion, determination of these gradients is sufficient.

Because $0 < \omega < \sqrt{2}$, the parameters (a, b) are both real and positive when $0 < c < c_b$. Thus, for subsonic sliding, boundedness of (A.2) for $y > 0$ requires that branch cuts $\mathrm{Im}(p) = 0$, $\mathrm{Re}(p) < 0$ and $\mathrm{Im}(p) = 0$, $\mathrm{Re}(p) > 0$ be introduced for the terms $\sqrt{\pm p}$, respectively, in order that $\mathrm{Re}(\sqrt{p}\sqrt{-p}) \geqslant 0$ in the cut plane. Substitution of (A.2) and (A.4) into $(\mathrm{A.1})_2$ and interchanging the order of the (t, p)-integrations reduces the inversion process to the generic integrals

$$\frac{1}{2\pi\mathrm{i}}\int\left(1, \frac{\sqrt{-p}}{\sqrt{p}}\right)\mathrm{e}^{p(x-t)-k\sqrt{p}\sqrt{-p}}\,\mathrm{d}p, \quad k = (\sqrt{\omega}ay, \sqrt{\omega}by). \tag{A.5}$$

The integrands are each analytic for $\mathrm{Re}(p) = 0$, so that the entire $\mathrm{Im}(p)$-axis can serve as the Bromwich contour. Performing the resulting integration produces the real integrals

$$\frac{1}{\pi}\int_0^\infty \mathrm{e}^{-kp}[\cos p(x-t), \sin p(x-t)]\,\mathrm{d}p \tag{A.6}$$

which, with the use of standard tables (Gradshteyn & Ryzhik, 1980), are

$$\frac{1}{\pi}\frac{(k, x-t)}{(x-t)^2 + k^2}. \tag{A.7}$$

In view of (A.2) and (A.7), the results

$$\begin{aligned}
\mu\frac{\partial u_1}{\partial x} &= \frac{\sqrt{\omega}ay}{\pi R}\int_L \sigma(t)\,\mathrm{d}t\left[\frac{K}{(t-x)^2 + \omega a^2 y^2} - \frac{2b^2}{(t-x)^2 + \omega b^2 y^2}\right], \\
\mu\frac{\partial u_2}{\partial x} &= \frac{a}{\pi R}\int_L \sigma(t)(t-x)\,\mathrm{d}t\left[\frac{\sqrt{\omega}K}{(t-x)^2 + \omega a^2 y^2} - \frac{2}{\sqrt{\omega}}\frac{1}{(t-x)^2 + \omega b^2 y^2}\right]
\end{aligned} \tag{A.8}$$

follow for $y > 0$.

For $c_b < c < c_a$ (transonic sliding speed) the parameter a in (A.3b) remains real and positive, but b is now imaginary. Therefore, the process used above must be modified to ensure that (A.2) remains bounded for $y > 0$. The integrations that result from application

of $(A.1)_1$ are similar in form, however, and it can be shown that

$$\begin{aligned}
\mu\frac{\partial u_1}{\partial x} &= \frac{a}{\pi R_-}\int_L \sigma(t)\left[\frac{4\beta}{\omega}(t-x)+\sqrt{\omega}K^3 y\right]\frac{\mathrm{d}t}{(t-x)^2+\omega a^2 y^2} \\
&\quad -\frac{2a\beta K^2}{\pi R_-}\int_L \frac{\sigma(t)\,\mathrm{d}t}{t-x-\sqrt{\omega}\beta y} - \frac{8a^2\beta^2}{\omega R_-}\sigma(x+\sqrt{\omega}\beta y), \\
\mu\frac{\partial u_2}{\partial x} &= \frac{\sqrt{\omega}Ka}{\pi R_-}\int_L \sigma(t)\left[\frac{4a^2\beta y}{\sqrt{\omega}}+K^2(t-x)\right]\frac{\mathrm{d}t}{(t-x)^2+\omega a^2 y^2} \\
&\quad +\frac{2aK^2}{\pi\sqrt{\omega}R_-}\int_L \frac{\sigma(t)\,\mathrm{d}t}{t-x-\sqrt{\omega}\beta y} + \frac{8a^2\beta}{\omega^{3/2}R_-}\sigma(x+\sqrt{\omega}\beta y)
\end{aligned} \tag{A.9}$$

for $y > 0$, where

$$\beta = \sqrt{c^2 - c_b^2}, \quad R_- = \left(K^2 - \frac{4}{\omega^2}\right)\left(K^2 - \frac{4}{3\omega^2}\right). \tag{A.10}$$

It is understood that the last terms in (A.9) appear only when $x + \sqrt{\omega}\beta y \in L$, and that the last integral terms then must be performed in the Cauchy principal value sense.

For $c > c_a$ (supersonic sliding speed), both (a, b) in (A.3a) are imaginary, but by the same procedures used above, application of $(A.1)_1$ to (A.2) can be shown to give

$$\begin{aligned}
\mu\frac{\partial u_1}{\partial x} &= \frac{K}{R_+}\sigma(x+\sqrt{\omega}\alpha y) - \frac{2\alpha\beta}{R_+}\sigma(x+\sqrt{\omega}\beta y), \\
\mu\frac{\partial u_2}{\partial x} &= \frac{\sqrt{\omega}K\alpha}{R_+}\sigma(x+\sqrt{\omega}\alpha y) + \frac{2\alpha}{\sqrt{\omega}R_+}\sigma(x+\sqrt{\omega}\beta y)
\end{aligned} \tag{A.11}$$

for $y > 0$. Here

$$\sqrt{3}\alpha = \sqrt{c^2 - c_a^2}, \quad R_+ = \frac{4}{\omega}\alpha\beta + K^2 \tag{A.12}$$

and it is understood that the first and second terms in both of (A.11) vanish unless $x + \sqrt{\omega}\alpha y \in L$ and $x + \sqrt{\omega}\beta y \in L$, respectively. This behaviour indicates that the half-space surface is deformed only within the contact zone.